Expression, Purification, and Characterization of *Mycobacterium tuberculosis* Mycothione Reductase[†]

Mehul P. Patel and John S. Blanchard*

Department of Biochemistry, Albert Einstein College of Medicine, 1300 Morris Park Avenue, Bronx, New York 10461

Received May 5, 1999; Revised Manuscript Received July 2, 1999

ABSTRACT: Mycothione reductase from the human pathogen *Mycobacterium tuberculosis* has been cloned, expressed in *Mycobacterium smegmatis*, and purified 145-fold to homogeneity in 43% yield. Amino acid sequence alignment of mycothione reductase with the functionally homologous glutathione and trypanothione reductase indicates conservation of the catalytically important redox-active disulfide, histidine−glutamate ion pair, and regions involved in binding both the FAD cofactor and the substrate NADPH. The homogeneous 50 kDa subunit enzyme exists as a homodimer and is NADPH-dependent and highly specific for the structurally unique low-molecular mass disulfide, mycothione, exhibiting Michaelis constants of 8 and 73 μM for NADPH and mycothione, respectively. HPLC analysis indicated the presence of 1 mol of bound FAD per monomer as the cofactor exhibiting an absorption spectrum with a λ_{max} at 462 nm with an extinction coefficient of 11 300 M^{-1} cm^{-1}. The reductive titration of the enzyme with NADH indicates the presence of a charge-transfer complex of one of the presumptive catalytic thiolates and FAD absorbing at ca. 530 nm. Reaction with serially truncated mycothione and other disulfides and pyridine nucleotide analogues indicates a strict minimal disulfide substrate requirement for the glucosamine moiety of mycothione. The enzyme exhibits bi-bi ping-pong kinetics with both disulfide and quinone substrates. Transhydrogenase activity is observed using NADH and thio-$NADP^+$, confirming the kinetic mechanism. We suggest mycothione reductase as the newest member of the class I flavoprotein disulfide reductase family of oxidoreductases.

Flavoprotein disulfide oxidoreductases represent a family of enzymes that catalyze redox reactions of critical cellular components. Low-molecular mass thiols are ubiquitously present in cells as mediators of cellular redox homeostasis and are maintained at high thiol:disulfide ratios by their cognate reductases. An abundant, structurally unique, low-molecular mass thiol has recently been identified in mycobacteria, and other actinomycetes, that does not resemble the tripeptide-based thiols, glutathione and trypanothione, or coenzyme A (*1*). This thiol, identified as a pseudodisaccharide consisting of a (α-1→1′) glycosidic linkage between D-glucosamine and *myo*inositol coupled via amide linkage to *N*-acetyl-L-cysteine, has been given the trivial name mycothiol, and we introduce mycothione as a shorthand name of the disulfide form (*2*) (Figure 1). Although structurally distinct from glutathione, which is not present in mycobacteria, mycothiol is posited to have a similar functional role in protection against oxidative stress derived from basal metabolic activities as well as from host−parasite confrontation. The biosynthesis of mycothiol has been delineated, and involves coupling of the cysteine α-carboxylate to the 2′-amine of the pseudodisaccharide followed by N-acetylation (*3*). The resurgence of tuberculosis has led to increased efforts to characterize the molecular mechanisms of drug resistance and pursue the identification of novel metabolic targets for chemotherapeutic intervention (*4*). Given the unique structure of mycothiol and its restricted prevalence among actinomycetales, the enzymes involved in mycothiol biosynthesis and metabolism appear to be promising targets for inhibitor development.

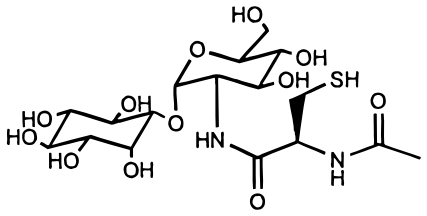

FIGURE 1: Structure of mycothiol.

Flavoprotein disulfide oxidoreductases constitute a class of flavoproteins that contain a redox-active disulfide involved in substrate disulfide reduction and include glutathione reductase, trypanothione reductase, lipoamide dehydrogenase,

[†] This work was supported by NIH Grant GM33449 and NIH Molecular Biophysics Training Program GM08572.

* Corresponding author. Phone: (718) 430-3096. Fax: (718) 430-8565. E-mail: blanchar@aecom.yu.edu.

[1] Abbreviations: MycR, mycothione reductase; TrpR, trypanothione reductase; GR, glutathione reductase; DTNB, 5,5′-dithiobis(2-nitrobenzoic acid); TEA, triethanolamine; Hepes, 4-(2-hydroxyethyl)-1-piperazineethanesulfonic acid; FAD, flavin adenine dinucleotide; FMN, flavin mononucleotide; β-NADPH, reduced β-nicotinamide adenine dinucleotide phosphate; β-NADH, reduced β-nicotinamide adenine dinucleotide; α-NADPH, reduced α-nicotinamide adenine dinucleotide phosphate; thio-NADPH, reduced β-thionicotinamide adenine dinucleotide phosphate; thio-NADH, reduced β-thionicotinamide adenine dinucleotide; 3APADH, reduced 3-acetylpyridine adenine dinucleotide; 3′-NADPH, reduced β-3′-nicotinamide adenine dinucleotide phosphate; NHDPH, reduced β-nicotinamide hypoxanthine dinucleotide phosphate; NHDH, reduced β-nicotinamide hypoxanthine dinucleotide; MSSM, mycothione (mycothiol disulfide); DI-MSSM, desmyoinositol mycothione; 2,6-DMBQ, 2,6-dimethylbenzoquinone.

10.1021/bi991025h CCC: $18.00
Published on Web 08/17/1999

and the high-molecular mass thioredoxin reductase identified in mammals (*5*, *6*). These enzymes have been isolated from prokaryotic and eukaryotic sources, and mechanistic studies in conjunction with the three-dimensional structural analysis of these enzymes indicate significant similarities in structure and mechanism. Glutathione and trypanothione reductase, which catalyze the pyridine nucleotide-dependent reduction of oxidized glutathione and trypanothione, respectively, are dimeric with approximate molecular masses of 50 000 Da and contain a single FAD[1] cofactor per monomer. They additionally both contain a flavin-proximal, redox-active disulfide that is reduced to the dithiol form during two-electron enzyme reduction to form a charge-transfer complex of the dithiol and FAD. Last, all contain a His−Glu ion pair involved in proton transfers accompanying disulfide substrate reduction (*7*). The demonstration of a mycobacterial-specific mycothione reductase activity (*8*) has motivated us to characterize this newly discovered reductase which exhibits no activity with the common naturally occurring disulfides, glutathione, trypanothione, and coenzyme A. An open reading frame for a putative glutathione reductase homologue from *Mycobacterium tuberculosis* H37Rv was identified as the result of the Sanger Centre genomic sequencing of this organism (*9*) (accession number AF002193). The translated amino acid sequence of the gene indicated the presence of all sequence elements involved in binding FAD and pyridine nucleotide, and both the redox-active dithiol and conserved His−Glu ion pair. Mycothiol has been shown to be present at millimolar levels in mycobacterial species and actinomycetes and to exhibit greater resistance to autoxidation than glutathione, providing a robust store of reducing equivalents (*10*). To date, the only other enzyme involved in the metabolic pathway of mycothiol that has been purified and characterized is the mycothiol-dependent formaldehyde dehydrogenase from the closely related Gram-positive *Rhodococcus erythropolis* (*11*).

We report here the cloning, expression, purification, and characterization of *M. tuberculosis* mycothione reductase. The *mtr*-encoded mycothione reductase is a homodimeric flavoprotein containing FAD as a cofactor. The enzyme exhibits a bi-bi ping-pong kinetic mechanism and possesses both transhydrogenase and diaphorase activities. Reductive titration of mycothione reductase indicates the presence of a charge-transfer complex of a thiolate and FAD in the two-electron reduced enzyme.

MATERIALS AND METHODS

Materials. Des*myo*inositol mycothiol was prepared as previously reported (*8*). Authentic mycothiol was a generous gift from D. J. Steenkamp (University of Cape Town Medical School, Cape Town, South Africa). Chromatography resins were obtained from Pharmacia. Nutrient media for growth of cells were from Fisher. All other reagents and enzymes were purchased from Sigma Chemical Co. Oligonucleotide primers were obtained from the Albert Einstein College of Medicine Oligonucleotide Facility.

Identification, Expression, Purification, and Sequencing of Mycothione Reductase. A search for a mycobacterial disulfide reductase was initiated by querying the Sanger Centre mycobacterial databank using the amino acid sequence of *Escherichia coli* glutathione reductase (accession number M13141). This query identified an amino acid sequence annotated as a glutathione reductase homologue as a translation product of gene Rv2855 found on the *M. tuberculosis* cosmid MTCY24A1. The identified open reading frame was used to design oligonucleotide primers for PCR amplification and cloning. The procedures for the cloning and construction of an expression system in *Mycobacterium smegmatis* for the *mtr* gene encoding mycothione reductase have been reported (*8*). The transformed *M. smegmatis* harboring the plasmid containing the *mtr* gene was grown in 5 L of Luria-Bertani medium containing 20 μg/mL kanamycin and 0.5% (v/v) Tween-80 at 37 °C until the OD_{600} reached 1.2, at which point the cultures were induced by heat shock and incubated at 45 °C until the OD_{600} reached 2.0. The cells were harvested by centrifugation and suspended (1:2 w:v) in 50 mM TEA-HCl (pH 7.6) containing 1 mM EDTA and a protease inhibitor cocktail (Boehringer Mannheim). The cells were lysed in a French pressure cell at 1200 psi. The cell-free extract, obtained by centrifugation, was made 1% in streptomycin sulfate by the addition of a 20% (w:v) streptomycin sulfate solution over the course of 30 min. The precipitate was removed by centrifugation and the supernatant dialyzed against 20 mM TEA-HCl (pH 7.6) at 4 °C. The precipitate produced during dialysis was removed by ultracentrifugation, and the clarified supernatant was applied to a 300 mL Fast-Flow Q-Sepharose anion exchange column that had been preequilibrated in 20 mM TEA-HCl (pH 7.6). The adsorbed protein was eluted with a 2 L linear 0 to 1 M NaCl gradient. Mycothione reductase activity was detected in fractions containing 0.55−0.65 M NaCl. The fractions containing activity were pooled and dialyzed overnight against 20 mM TEA-HCl (pH 7.6) at 4 °C. The dialysate was concentrated to 20 mL in an Amicon pressure filtration cell using a 10 000 Da cutoff filter. The protein solution was applied in three aliquots to a 20 mL 2′,5′-ADP−Sepharose 4B column previously equilibrated in 20 mM TEA-HCl (pH 7.6). Following a wash with 50 mL of 20 mM TEA-HCl (pH 7.6) to remove nonadsorbed proteins, a 200 mL linear 0 to 1 M NaCl gradient eluted mycothione reductase at 0.1 M NaCl. Three proteins corresponding to monomer molecular masses of 45, 50, and 100 kDa were present in the fractions containing mycothione reductase activity, as determined by SDS−PAGE. *M. tuberculosis* mycothione reductase was further purified on a 5 mL MonoQ column preequilibrated in 20 mM TEA-HCl (pH 7.6). A 250 mL 0 to 1 M NaCl gradient eluted mycothione reductase activities at 0.45 and 0.50 M NaCl. SDS−PAGE analysis indicated the presence of the 45 kDa protein in the 0.45 M eluant and the 50 kDa protein in the 0.50 M eluant. The 50 kDa protein was the desired recombinant *M. tuberculosis* expression product, and the 45 kDa protein was the constitutively expressed *M. smegmatis* mycothione reductase. Fractions containing either the *M. tuberculosis* or *M. smegmatis* mycothione reductase activity were individually pooled, determined to be >95% pure by SDS−PAGE, and stored in 50% glycerol at −20 °C. Protein concentrations were determined by the Bradford dye-binding assay (Bio-Rad) using bovine serum albumin as a standard, and the concentration of mycothione reductase was determined by measuring the absorbance of enzyme-bound FAD at 462 nm using an extinction coefficient of 11 300 M^{-1} cm^{-1} (*12*). The apparent native molecular mass of mycothione reductase from *M. tuberculosis* was determined on a Super-

dex 200 gel filtration column (Pharmacia) calibrated with molecular mass standards (Bio-Rad). The *M. tuberculosis* mycothione reductase coding sequence of the PCR-amplified pMV261-MR was completely sequenced with a PRISM Dyedeoxy Terminator Cycle Sequencing kit and sequencer (Applied Biosystems, Inc.) at the Albert Einstein College of Medicine Sequencing Facility. Amino terminal sequencing of the purified *M. tuberculosis* and *M. smegmatis* was performed with an Applied Biosystems sequencer using standard Edman chemistry (20 cycles). The Gap algorithm was used for amino acid sequence comparisons using the blossom62 scoring matrix (gap creation penalty of 8 and gap extension penalty of 2). Multiple amino acid sequence alignments were generated using the Pileup function of the SeqWeb network service using the same constraints that were imposed for the Gap analysis (GCG Wisconsin Package).

Spectra of Mycothione Reductase and Anaerobic Reductive Titration with NADH. Mycothione reductase was reduced under anaerobic conditions with NADH. Solutions contained 28 μM enzyme in 50 mM Hepes (pH 7.6) containing 0.1 mM EDTA at 4 °C. The enzyme solution was made anaerobic in a quartz cuvette fitted with a septum cap by purging with nitrogen for 30 min. Titrations with an anaerobic solution of NADH containing 1 equiv/10 μL were carried out using a gastight Hamilton syringe. Spectra were recorded using a UVIKON-9310 spectrophotometer.

Cofactor Identification. Native mycothione reductase was heated at 100 °C for 10 min, and the denatured protein was removed by filtration on a 10 kDa cutoff spin filter (Millipore). The eluant was purified by HPLC on an analytical Waters reverse-phase μBondapack C-18 support using a 30 min linear 0 to 50% methanol gradient, and the results were compared to the elution profiles of FAD, FMN, and riboflavin standards which were detected at 460 nm.

Enzyme Kinetics. Mycothione reductase activity was assayed spectrophotometrically by monitoring the des*myo*-inositol mycothione- or quinone-dependent oxidation of NADPH at 340 nm ($\epsilon = 6220$ M^{-1} cm^{-1}) in 50 mM Hepes (pH 7.6) containing 0.1 mM EDTA using a UVIKON-9310 spectrophotometer. The oxidation of pyridine nucleotide analogues was monitored at the following wavelengths and with the following extinction coefficients: NADH, NHDH, NHDPH, and 3′NADPH, 340 nm ($\epsilon = 6220$ M^{-1} cm^{-1}); tNADH and tNADPH, 395 nm ($\epsilon = 11\,300$ M^{-1} cm^{-1}); and 3APADH, 363 nm ($\epsilon = 9100$ M^{-1} cm^{-1}). The NADPH-dependent reduction of DTNB was monitored at 412 nm ($\epsilon = 13\,600$ M^{-1} cm^{-1}). Kinetic parameters were determined using initial rate assays, and the data were fit to the nonlinear fitting programs of Cleland (*13*). Individual saturation curves were fitted to eq 1

$$v = VA/(K + A) \quad (1)$$

where A is the variable substrate concentration. Parallel initial velocity patterns were fitted to eq 2

$$v = VAB/(K_aB + K_bA + AB) \quad (2)$$

where A and B, and K_a and K_b, are the concentrations, and Michaelis constants, respectively, for the substrates. The transhydrogenase assay contained 100 μM NADH and 500 μM thio-NADP$^+$ in 50 mM Hepes (pH 7.6) containing 0.1 mM EDTA and using a reference containing the same mixture but lacking enzyme. Transhydrogenase activity was determined by measuring the UV−visible spectrum between 300 and 525 nm.

Iodoacetamide Inactivation. Alkylation of mycothione reductase with iodoacetamide was performed under anaerobic conditions, as described above, in solutions containing 0.5 mM NADPH and 25 μg of mycothione reductase in 50 mM Hepes (pH 7.6) and 0.1 mM EDTA. An anaerobic solution of 100 mM iodoacetamide was added to the reduced mycothione reductase solution to a final concentration of 1 mM with a gastight Hamilton syringe, and the reaction was allowed to proceed for 80 min. Reductase and diaphorase activity measurements were performed as a function of the length of time of the incubation with iodoacetamide.

RESULTS AND DISCUSSION

Pathogenic mycobacteria undergo an intracellular phase as part of its infective cycle whereby they are phagocytized by host immune cells, such as macrophages, and are subjected to oxidative insult by these cells. They both survive this oxidative onslaught and replicate within the phagolysosomal vesicle. The structurally unique, low-molecular mass thiol mycothiol has been identified in mycobacteria, which lack both glutathione and glutathione reductase, at millimolar levels (*14*). The desirability of maintaining a high thiol:disulfide ratio within the mycobacterial cell to prevent oxidative injury and maintain a reducing intracellular environment suggests an important role for the reductase. The lack of glutathione reductase activity in mycobacterial cell-free lysates (*8*) suggested the presence of a mycothione-specific reductase functionally analogous to the ubiquitous glutathione reductase.

Cloning and Sequence Analysis of M. tuberculosis Mycothione Reductase. The search for a mycobacterial disulfide reductase in the *M. tuberculosis* Sanger database using the functionally homologous *E. coli* glutathione reductase sequence as a query resulted in a match with an open reading frame in the genome of *M. tuberculosis* containing significant stretches of identity with members of pyridine nucleotide-dependent disulfide oxidoreductases. The amino acid sequence of this putative gene product is relatively identical with those of *Crithidia fasciculata* trypanothione reductase (28%) and human glutathione reductase (31%) (Figure 2). Sequence comparison of the putative mycobacterial flavoprotein disulfide reductase with the members of this family indicates the presence of the conserved redox-active cysteines (CXXXXC) and a nucleotide-binding motif (GXGXXN) near the amino terminus for binding the ADP moiety of FAD. The C-terminal redox-active cysteine of human glutathione reductase has been shown to form a charge-transfer complex with the oxidized flavin in the two-electron reduced form of the enzyme, and the N-terminal cysteine nucleophilically attacks the disulfide substrate, initiating disulfide substrate reduction (*15*). A pyridine nucleotide-binding motif (YYGX-GXXA, where Y is apolar) is evident between residues 179 and 184 of the polypeptide chain. The terminal alanine residue in this motif has been associated with disruption of the close packing of the secondary structural elements for accommodating the 2′-phosphate of NADPH (*16*). This sequence motif explains the kinetic behavior exhibited by mycothione reductase with the 2′-phosphorylated nucleotide analogues (see below). The tyrosine residue (Y197 of human

```
C. fas. TrpR  ~~~~~~~~~~ ~~~~~~MSRA YDLVVIGAGS GRLEAGWNAA SLHKKRVAVI DLQKHHGPPH YAALGGTCVN  54
Human GR      ACRQEPQPQG PPPAAGAVAS YDYLVIGGGS GGLASARRAA EL.GARAAVV ESHK..... ...LGGTCVN  60
M. tub. MycR  ~~~~~~~~~~ ~~~~~~~MET YDIAIIGTGS GNSILDERYA S...KRAAIC E......... QGTFGGTCLN  41
Consensus     ---------- ---------- YD---IG-GS G--------A -----R-A-- ---------- ----GGTC-N

C. fas. TrpR  VGCVPKKLMV TGANYMDTIR ESAGFGWELD RESVRPNWKA LIAA...KNK AVSGINDSYE GMFADTEGLT  121
Human GR      VGCVPKKVMW NTAVHSEFMH DHADYGFP.S CEG.KFNWRV IKEK...RDA YVSRLNAIYQ NNLTKSH.IE  124
M. tub. MycR  VGCIPTKMFV YAAEVAKTIR GASRYGIDAH IDRVR..WDD VVSRVFGRID PIALSGEDYR RCAPNIDVYR  109
Consensus     VGC-P-K--- --A------- -----G---- -------W-- ---------- --------Y- ----------

C. fas. TrpR  FHQGFGALQD NHTVLVRESA DPNSAVLETL DTEYILLATG ...SWPQHLG IEGDDLCITS NEAFYLDEAP  188
Human GR      IIRGHAAFTS DPKPTIEVSG KKYTA..... ..PHILIATG GMPSTPHESQ IPGASLGITS DGFFQLEELP  187
M. tub. MycR  THTRFGPVQA DGRYLLRTDA G......EEF TAEQVVIAAG SRPVIPPAIL ASGVDYH.TS DTVMRIAELP  172
Consensus     ---------- ---------- ---------- -------A-G -----P---- --G-----TS -------E-P

C. fas. TrpR  KRALCVGGGY ISIEFAGIFN AYKARGGQVD LAYRGDMILR GFDSELRKQL TEQLRANGIN VRTHENPAKV  258
Human GR      GRSVIVGAGY IAVEMAGILS AL...GSKTS LMIRHDKVLR SFDSMISTNC TEELENAGVE VLKFSQVKEV  254
M. tub. MycR  EHIVIVGSGF IAAEFAHVFS AL...GVRVT LVIRGSCLLR HCDDTICERF T.RIASTKWE LRTHRNVVDG  238
Consensus     -----VG-G- I--E-A---- A----G---- L--R----LR --D------- T--------- ----------

C. fas. TrpR  TKNADG..TR HVVFESG... ...AEADYDV VMLAIGRVPR SQTLQLEKAG VEVAKNGAIK VDAYSKTNVD  320
Human GR      KKTLSGLEVS MVTAVPGRLP VMTMIPDVDC LLWAIGRVPN TKDLSLNKLG IQTDDKGHII VDEFQNTNVK  324
M. tub. MycR  QQRGSGVALR ...LDDG... ...CTINADL LLVATGRVSN ADLLDAEQAG VDVED.GRVI VDEYQRTSAR  298
Consensus     -----G---- ------G--- --------D- ---A-GRV-- ---L-----G ------G--- VD----T---

C. fas. TrpR  NIYAIGDVTD RVMLTPVAIN EGAAFVDTVF ANKPRA.... .TDHTKVACA VFSIPPMGVC GYVEEDAAKK  385
Human GR      GIYAVGDVCG KALLTPVAIA AGRKLAHRLF EYKEDSK... .LDYNNIPTV VFSHPPIGTV GLTEDEAIHK  390
M. tub. MycR  GVFALGDVSS PYLLKHVANH EARVVQHNLL CDWEDTQSMI VTDHRYVPAA VFTDPQIAAV GLTENQAVAK  368
Consensus     ---A-GDV-- ---L--VA-- ---------- ---------- --D------- VF--P----- G--E--A--K

C. fas. TrpR  Y..DQVAVYE SSFTPLMHNI SGSTYKKFMV RIVTNHADGE VLGVHMLGDS SPEIIQSVAI CLKMGAKISD  453
Human GR      YGIENVKTYS TSFTPMYHAV T.KRKTKCVM KMVCANKEEK VVGIHMQGLG CDEMLQGFAV AVKMGATKAD  459
M. tub. MycR  .GLD.ISVKI QDYGDVAYGW AMED.TSGIV KLITERGSGR LLGAHIMGYQ ASSLIQPLIQ AMSFGLTAAE  435
Consensus     ---------- ---------- ---------- ---------- --G-H--G-- -----Q---- ----G-----

C. fas. TrpR  V.YNTIGVHP TSAE....EL CSMRTPAYFY EKGKRVEKID SNL                              491
Human GR      F.DNTVAIHP TSSE....EL VTLR~~~~~~ ~~~~~~~~~~ ~~~                             479
M. tub. MycR  MARGQYWIHP ALPEVVENAL LGLR~~~~~~ ~~~~~~~~~~ ~~~                             459
Consensus     --------HP ---E-----L ---R------ ---------- ---
```

FIGURE 2: Amino acid sequence alignment of *M. tuberculosis* mycothione reductase with *C. fasciculata* trypanothione reductase and human glutathione reductase. Identical residues in all three sequences are bold. Gaps introduced using the algorithm of the program Pileup are represented by dots.

glutathione reductase) found in the nucleotide-binding domain of the flavoprotein reductases is substituted with a phenylalanine residue in mycothione reductase. The catalytically essential His-444−Glu-449 ion pair near the carboxy terminus is also present in mycothione reductase. These residues, in functionally homologous reductases, have been shown to function in proton transfer to the leaving substrate thiolate (*17*).

Expression, Purification, and Amino-Terminal Sequencing of M. tuberculosis Mycothione Reductase. An expression system using the mycobacterial heat-shock protein (hsp60) sensitive vector, designated pMV261-MR, and *M. smegmatis* as a host has yielded soluble mycothione reductase. The level of expression of the *M. tuberculosis* mycothione reductase was 6-fold greater than the constitutive level of expression of the *M. smegmatis* reductase, similar to expression levels reported previously (*8*). Mycothione reductase from *M. tuberculosis* was purified 145-fold in 43% overall yield (Table 1). Purification via streptomycin sulfate fractionation and sequential chromatography on Q-Sepharose, 2′,5′-ADP−Sepharose, and Mono-Q yielded a solution exhibiting a single band at 50 kDa on SDS−PAGE, and the apparent native molecular mass, determined by gel filtration, was ca. 100 000 Da (data not shown), indicating a dimeric state for the reductase under nondenaturing conditions as is true for all members of this enzyme family. The enzyme copurified on 2′,5′-ADP−Sepharose with two other contaminants, 45 and 100 kDa proteins, both of which were subsequently separated by high-resolution anion exchange chromatography. The 45 kDa protein exhibited mycothione reductase activity and is likely to be the constitutively expressed *M. smegmatis* mycothione reductase (no amino acid sequence has been reported for the *M. smegmatis* MycR). The homogeneous 50 kDa *M. tuberculosis* mycothione reductase used for the studies described in this paper was subjected to amino-terminal Edman degradation. The 11-residue amino-terminal sequence of the purified enzyme (METYDIAIIGT) matches that of the translated nucleotide sequence of the *mtr* gene.

Table 1: Purification of *M. tuberculosis* Mycothione Reductase

pooled fraction	total protein (mg)	total activity (units)	specific activity (units/mg)	yield (%)	purification (*x*-fold)
crude dialysate	986	24.3	0.025	100	−
Q-Sepharose	89	16.2	0.180	67	7.2
2′,5′-ADP− Sepharose 4B	4.4	12.7	2.89	52	116
Mono-Q	2.9	10.5	3.63	43	145

Spectral Characterization. The visible absorption spectra of oxidized mycothione reductase indicate the presence of a flavin cofactor as observed for other flavoproteins (*7*), with

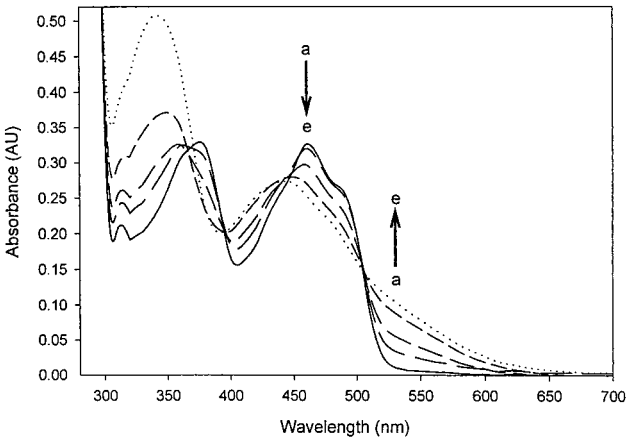

FIGURE 3: Anaerobic titration of 28 μM mycothione reductase with NADH. The number of equivalents of NADH used to obtain the spectral changes was (a) 0, (b) 0.25, (c) 0.5, (d) 1, and (e) 2.

absorbance maxima at 278, 377, and 462 nm with a shoulder at ca. 485 nm (Figure 3). The ratio of absorbances (A_{278}/A_{462}) determined for the enzyme of 6.2 is similar to the value observed for other flavoprotein reductases (*18*−*20*). The value of this ratio also indicates the absence of bound $NADP^+$ in the purified preparation, compared to flavoprotein reductases that have a higher affinity for $NADP^+$ such as trypanothione reductase and mercuric reductase (*19*, *21*) and are purified with bound $NADP^+$.

The flavin present in mycothione reductase was shown to be FAD by thermal denaturation of the enzyme. The liberated flavin cofactor was analyzed by HPLC and shown to coelute with a commercial preparation of FAD with a retention time of 6.5 min. Riboflavin and FMN, used as standards for comparison, eluted with retention times of 18.8 and 8.4 min, respectively.

Reductive Titration of Mycothione Reductase. The presence of a charge-transfer complex of FAD and the putative proximal thiolate of the redox pair was investigated by reductive titration of oxidized mycothione reductase under anaerobic conditions (Figure 3). The spectrum of the enzyme, upon titration with NADH, exhibits decreases in absorbance at 462 nm and increases at ca. 530 nm, demonstrating the formation of the hallmark charge-transfer complex observed in these flavoprotein reductases. NADH was used in these reductions instead of NADPH to decrease the likelihood of formation of reduced enzyme−nucleotide complexes. Complete four-electron reduction of the enzyme could not be achieved even with excess NADH. However, the lack of an isosbestic point between the spectra for mycothione reductase reduced with 2 equiv of NADH and the other spectra suggests the formation of an EH_2−NADH complex from EH_2.

Reductive Alkylation. The involvement of the putative redox-active cysteines (C39 and C44) of mycothione reductase in its catalytic mechanism was probed by reductive alkylation with iodoacetamide under anaerobic conditions (Figure 4). The mycothione reductase activity of the enzyme decreased over the time course of inactivation with a half-life of ca. 21 min. The diaphorase activity of mycothione reductase was unaffected by alkylation, suggesting that the redox-active cysteines are not involved in quinone reduction, as has been observed with trypanothione and glutathione reductases (*22*, *23*).

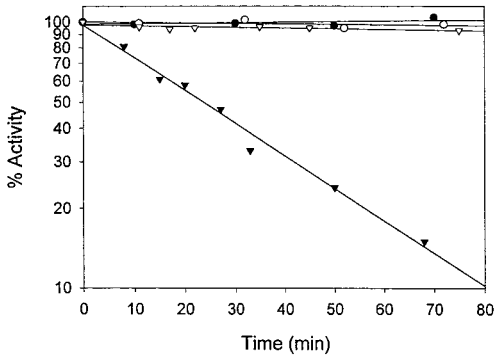

FIGURE 4: Iodoacetamide inactivation of mycothione reductase as a function of time. The NADPH-dependent reductase activity of nonalkylated mycothione reductase with DI-MSSM (●) and 2,6-DMBQ (○) and iodoacetamide-incubated enzyme with DI-MSSM (▼) and 2,6-DMBQ (▽).

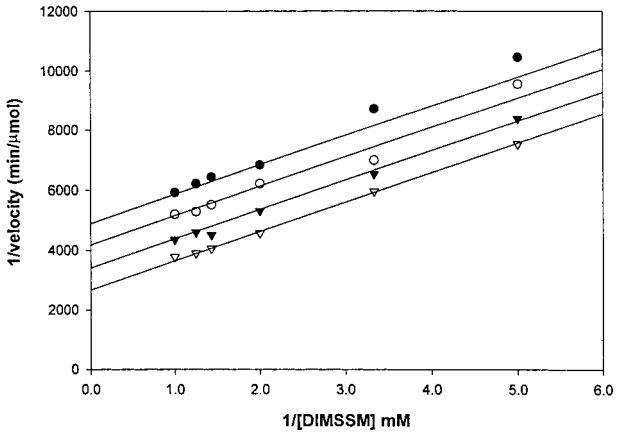

FIGURE 5: Initial rate analysis of the bisubstrate reaction mechanism of mycothione reductase. The lines represent fits of each set of data to eq 1. The data points that are shown were determined experimentally. Each set of data represents the following NADPH concentrations: 5.0 (●), 6.6 (○), 10 (▼), and 20 μM (▽).

Steady-State Kinetics. M. tuberculosis mycothione reductase exhibited the largest *V*/*K* values for mycothione and NADPH. Because of the limited quantities of the physiological disulfide substrate, des*myo*inositol mycothione, a synthetic analogue, was used to determine the kinetic mechanism. Initial rates, obtained by varying the concentration of the disulfide substrate at several fixed concentrations of NADPH, exhibit a parallel initial velocity pattern, indicative of a bi-bi ping-pong kinetic mechanism (Figure 5). This kinetic mechanism was confirmed by analyzing the transhydrogenase activity of the reductase, which measures the rate of enzyme-mediated hydride exchange between NADH and thio-$NADP^+$ (Figure 6).

A parallel initial velocity pattern was also observed using NADH and 2,6-dimethylbenzoquinone as substrates. For other flavoprotein reductases, reduction of quinones has been demonstrated to proceed via one-electron reduction at a site distinct from those involved in hydride ion transfer and disulfide reduction (*23*). Taken together, the results of these initial velocity experiments and transhydrogenase activity and reductive alkylation studies suggest a kinetic mechanism in which, in the first half-reaction, NADPH reduces FAD, which subsequently transfers reducing equivalents to the redox-active disulfide to generate the stable two-electron reduced enzyme shown in Scheme 1. The two-electron

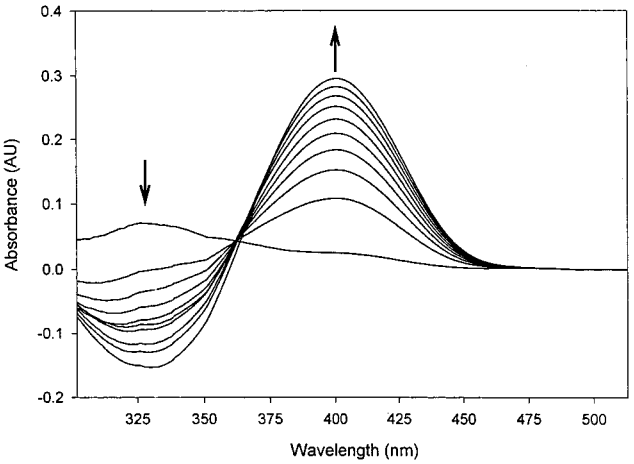

FIGURE 6: Demonstration of transhydrogenase activity between NADH and thio-NADP$^+$ by mycothione reductase. The reaction was monitored for 100 min, and spectra were recorded at 10 min intervals.

Scheme 1: Minimal Chemical Mechanism of Mycothione Reductase

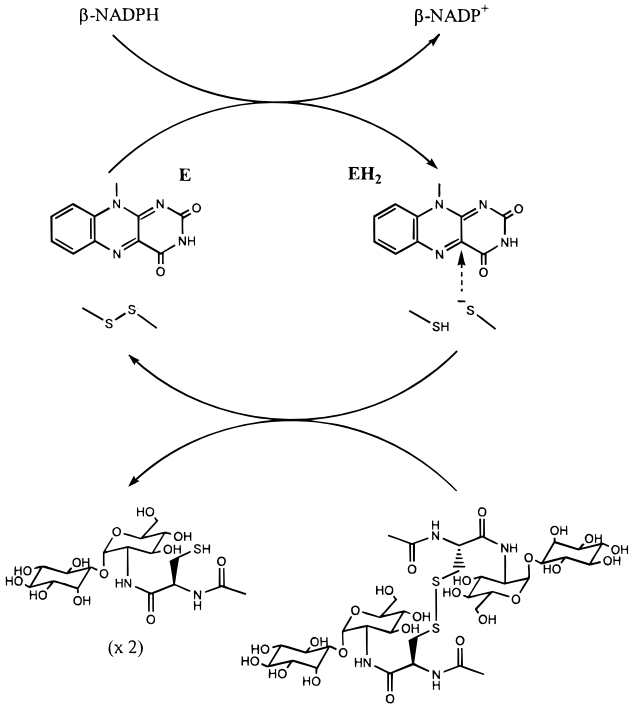

reduced enzyme in turn reduces the disulfide substrate via dithiol−disulfide interchange in the second half-reaction.

Substrate Specificity. The interaction of substrate analogues with mycothione reductase was examined by determining the steady-state kinetic parameters for pyridine nucleotide, disulfide, and quinone substrates (Tables 2 and 3). The k_{cat} for the enzyme using the physiological substrates is 400 mol of MSSM per mole of FAD per minute, a value that is 1−2 orders of magnitude lower than that observed for homologous disulfide reductases from faster growing organisms. A low intrinsic activity has been observed for other mycobacterial enzymes, including the related flavoproteins thioredoxin reductase and lipoamide dehydrogenase (*24*, *25*). Given the slow autoxidation rate of mycothiol compared to those of cysteine and glutathione (*10*), the lower rate of catalytic turnover of mycothione reductase may be sufficient to maintain intracellular reduced thiol at millimolar levels. The Michaelis constants measured for mycothione and NADPH of 70 and 8 μM, respectively, are similar to those of the corresponding substrates of glutathione and trypanothione reductase. The 2′-phosphorylated nucleotide substrate NADPH is preferred over NADH for most disulfide reductases that have been studied (*7*). For mycothione reductase, a modest 13-fold preference, based on *V*/*K* values, for NADPH over NADH is observed. This preference is possibly due to the presence of R203 and R209 in mycothione reductase, which are homologous to residues in other NADPH-selective reductases that have been shown to be involved in electrostatic interactions with the 2′-phosphoryl group of the pyridine nucleotide (*26*). 3′-NADPH exhibits no activity with mycothione reductase, indicating a strict preference for the 2′-phosphate regioisomer. Thio-NADPH exhibits a 9-fold lower K_m value and an 11-fold lower *V* compared to those of β-NADPH. The more positive redox potentials of thio-NAD(P)H and 3APADH are likely to be a contributing factor in the lower relative *V* observed for these analogues. The higher apparent Michaelis constant of 3APADH suggests specific interactions with the nicotinamide carboxamido functionality for efficient binding. The hypoxanthine analogue, NHDPH, exhibits the same maximum velocity as NADPH, and the K_m for NHDPH is only 3-fold greater than that for NADPH. The adenine-binding region is relatively solvent-exposed in the related glutathione reductase (*26*).

Disulfide substrates that are serially truncated and represent a partial spectrum of mycothione analogues have also been

Table 2: Kinetic Parameters of Substrates for *M. tuberculosis* Mycothione Reductase

nucleotide substrate[a]	K_m (μM)	V_{rel}[b] (%)	$(V/K)_{rel}$ (%)
β-NADPH	7.7 ± 0.5	100	100
NHDPH	23 ± 1	100	33
NADH	43 ± 6	44	8
NHDH	200 ± 30	39	1.5
thio-NADPH	0.9 ± 0.1	14	114
thio-NADH	90 ± 20	9	7
α-NADPH	55 ± 10	2	0.3
3APADH[c]	–	–	–
3′-NADPH[d]	–	–	–
disulfide substrate[e]	**K_m (μM)**	**V_{rel}[b] (%)**	**$(V/K)_{rel}$ (%)**
MSSM	70 ± 30	100	100
DI-MSSM	510 ± 40	45	6
DTNB	3300 ± 700	3	0.0007

[a] Determined using 800 μM DI-MSSM. [b] Relative to that substrate exhibiting the highest activity in its substrate class. [c] A linear increase in activity was observed at a nucleotide concentration of 1.5 mM with increasing standard error. A concentration of 2 mM resulted in an absorbance the was too high for measuring the small change in activity. [d] No activity was observed at a nucleotide concentration of 200 μM. [e] Determined using 200 μM β-NADPH.

Table 3: Kinetic Parameters of Quinone Substrates for *M. tuberculosis* Mycothione Reductase

quinone substrate[a] (E^1, mV)	K_m (μM)	V_{rel}[b] (%)	$(V/K)_{rel}$ (%)
2,6-dimethylbenzoquinone (−80)	4000 ± 800	100	100
5-hydroxy-1,4-naphthoquinone (−90)	540 ± 60	67	496
5,8-dihydroxy-1,4-naphthoquinone (−110)	340 ± 80	55	647
2-methyl-1,4-naphthoquinone (−200)	240 ± 50	3	50

[a] Determined using 200 μM β-NADPH. [b] Relative to that substrate exhibiting the highest activity in its substrate class.

subjected to kinetic analysis so a better understanding of the specificity of mycothione reductase for this novel disulfide could be obtained. The data in Table 2 indicate the absolute requirement for the glucosamine moiety in the mycothiol substrate for activity, and the *V*/*K* value of des*myo*inositol mycothione is 6% of that of authentic mycothione. The free acid and *O*-methyl ester forms of *N*-acetyl-L-cystine exhibit no activity. The aromatic disulfide, DTNB, exhibits modest activity with mycothione reductase.

Quinone substrates that have been shown to react with various flavoproteins have been assessed for their reactivity with mycothione reductase (Table 3). The values of *V* for all of the quinone substrates that were tested, except 2-methyl-1,4-naphthoquinone, are greater than that for the physiological substrate, mycothione. These data also indicate a correlation between the single-electron reduction potential (E^1) and the maximum velocity of reduction of these substrates. The retention of diaphorase activity observed upon active-site thiol alkylation indicates quinone reduction does not involve the redox-active cysteines.

The initial kinetic characterization presented here allows us to present a minimal chemical mechanism for the reaction of *M. tuberculosis* mycothione reductase as shown in Scheme 1. The transfer of a hydride ion from NAD(P)H to FAD in oxidized mycothione reductase (E) generates the spectroscopically observable reduced form of the enzyme (EH_2), comprising the reductive half-reaction. The two-electron reduced enzyme (EH_2) reduces the disulfide substrate, yielding two molecules of thiol product and regenerating oxidized enzyme (E), which constitutes the oxidative half-reaction.

The significant sequence and physical similarities between mycothione reductase and glutathione reductase and trypanothione reductase identify it as a new member of the class I flavoprotein disulfide reductase. This initial characterization of mycothione reductase allows us to focus our efforts on a more detailed analysis of the structure and chemical mechanism of the enzyme. The strict specificity for mycothione, and the lack of activity with glutathione or trypanothione (*8*), suggests that mycothione reductase presents a suitable target for the development of antimicrobial agents against pathogenic actinomycetales. The presumed similar roles of mycothione reductase, trypanothione reductase, and glutathione reductase may suggest a susceptibility of mycothione reductase toward flavoprotein reductase mechanism-based inhibitors. Quinone-based "subversive substrates" have been shown to effectively inhibit trypanothione reductase activity via a redox-cycling event (*27*). The demonstration here of robust quinone reductase activity may permit a similar strategy in the design of inhibitors against mycothione reductase. A rational approach in the design of such antitubercular agents will be aided by the determination of the three-dimensional structure of mycothione reductase. Efforts aimed at this are currently underway, and will broaden our understanding of mycothione reductase and its relationship with other flavoprotein reductases.

ACKNOWLEDGMENT

We thank Dr. Daniel J. Steenkamp for supplying authentic mycothione. We also thank Mr. Renjian Zheng for technical assistance with molecular biology.

REFERENCES

1. Sakuda, S., Zhou, Z.-Y., and Amada, Y. (1994) *Biosci., Biotechnol., Biochem. 58*, 1347−1348.
2. Spies, H. S. C., and Steenkamp, D. J. (1994) *Eur. J. Biochem. 224*, 203−213.
3. Bornemann, C., Jardine, M. A., Spies, H. S. C., and Steenkamp, D. J. (1997) *Biochem. J. 325*, 623−629.
4. Young, D. B., and Duncan, K. (1995) *Annu. Rev. Microbiol. 49*, 641−673.
5. Zhong, L., Arnér, E. S. J., Ljung, L., Åslund, F., and Holmgren, A. (1998) *J. Biol. Chem. 273*, 8581−8591.
6. Arscott, L. D., Gromer, S., Schirmer, R. H., Becker, K., and Williams, C. H., Jr. (1997) *Proc. Natl. Acad. Sci. U.S.A. 94* (8), 3621−3626.
7. Williams, C. H., Jr. (1992) in *Chemistry and Biochemistry of Flavoenzymes* (Müller, F., Ed.) Vol. III, pp 121−195, CRC Press, Boca Raton, FL.
8. Patel, M. P., and Blanchard, J. S. (1998) *J. Am. Chem. Soc. 120*, 11538−11539.
9. Cole, S. T., Brosch, R., Parkhill, J., Garnier, T., Churcher, C., Harris, D., Gordon, S. V., Eiglmeier, K., Gas, S., Barry, C. E., III, Tekaia, F., Badcock, K., Basham, D., Brown, D., Chillingworth, T., Connor, R., Davies, R., Devlin, K., Feltwell, T., Gentles, S., Hamlin, N., Holroyd, S., Hornsby, T., Jagels, K., Krogh, A., Mclean, J., Moule, S., Murphy, L., Oliver, K., Osborne, J., Quail, M. A., Rajandream, M.-A., Rogers, J., Rutter, S., Seeger, K., Skelton, J., Squares, S., Sulston, J. E., Taylor, K., Whitehead, S., and Barrell, B. G. (1998) *Nature 393*, 537−544.
10. Newton, G. L., Bewley, C. A., Dwyer, T. J., Horn, R., Aharonowitz, Y., Cohen, G., Davies, J., Faulkner, D. J., and Fahey, R. C. (1995) *Eur. J. Biochem. 230*, 821−825.
11. Eggeling, L., and Sahm, H. (1985) *Eur. J. Biochem. 150*, 129−134.
12. Whitby, L. G. (1953) *Biochem. J. 54*, 437−442.
13. Cleland, W. W. (1979) *Methods Enzymol. 63*, 103−138.
14. Newton, G. L., Arnold, K., Price, M. S., Sherrill, C., Delcardayre, S. B., Aharonowitz, Y., Cohen, G., Davies, J., Fahey, R. C., and Davis, C. (1996) *J. Bacteriol. 178*, 1990−1995.
15. Arscott, L. D., Thorpe, C., and Williams, C. H., Jr. (1981) *Biochemistry 20*, 1513−1520.
16. Rao, S. T., and Rossman, M. G. (1973) *J. Mol. Biol. 76*, 241−256.
17. Wong, K. K., Vanoni, M. A., and Blanchard, J. S. (1988) *Biochemistry 27*, 7091−7096.
18. Massey, V., and Williams, C. H., Jr. (1965) *J. Biol. Chem. 240*, 4470−4480.
19. Fox, B., and Walsh, C. T. (1982) *J. Biol. Chem. 257*, 2498−2503.
20. Sullivan, F. X., Shames, S. L., and Walsh, C. T. (1989) *Biochemistry 28*, 4986−4992.
21. Shames, L. S., Fairlamb, A. H., Cerami, A., and Walsh, C. T. (1986) *Biochemistry 25*, 3519−3526.
22. Cènas, N. K., Rakauskienè, G. A., and Kulys, J. J. (1989) *Biochim. Biophys. Acta 973*, 399−404.
23. Cenas, N. K., Arscott, D., Williams, C. H., Jr., and Blanchard, J. S. (1994) *Biochemistry 33*, 2509−2515.
24. Marcinkeviciene, J., and Blanchard, J. S. (1997) *Arch. Biochem. Biophys. 340*, 169−176.
25. Wang, P.-F., Marcinkeviciene, J., Williams, C. H., Jr., and Blanchard, J. S. (1998) *Biochemistry 37*, 16378−16389.
26. Pai, E. F. (1988) *Biochemistry 27*, 4465−4474.
27. Henderson, G. B., Ulrich, P., Fairlamb, A. H., Rosenberg, I., Pereira, M., Sela, M., and Cerami, A. (1988) *Proc. Natl. Acad. Sci. U.S.A. 85*, 5374−5378.

BI991025H